



Fermi National Accelerator Laboratory

FERMILAB-Conf-96/062

REVISED

**Comparison of Backgrounds in Detectors for
LHC, NLC and $\mu^+\mu^-$ Colliders**

N.V. Mokhov

*Fermi National Accelerator Laboratory
P.O. Box 500, Batavia, Illinois 60510*

April 1996

*Proceedings of the Symposium on Physics Potential and Development of $\mu^+\mu^-$ Colliders,
San Francisco, California, December 13-15, 1995*

Disclaimer

This report was prepared as an account of work sponsored by an agency of the United States Government. Neither the United States Government nor any agency thereof, nor any of their employees, makes any warranty, expressed or implied, or assumes any legal liability or responsibility for the accuracy, completeness, or usefulness of any information, apparatus, product, or process disclosed, or represents that its use would not infringe privately owned rights. Reference herein to any specific commercial product, process, or service by trade name, trademark, manufacturer, or otherwise, does not necessarily constitute or imply its endorsement, recommendation, or favoring by the United States Government or any agency thereof. The views and opinions of authors expressed herein do not necessarily state or reflect those of the United States Government or any agency thereof.

Comparison of backgrounds in detectors for LHC, NLC and $\mu^+\mu^-$ colliders

N. V. Mokhov*

Fermi National Accelerator Laboratory, P. O. Box 500, Batavia, IL 60510, U. S. A.

Background levels in detectors at future high-luminosity colliders of three different types - pp , e^+e^- and $\mu^+\mu^-$ - are analyzed. Two sources - debris from the collision points and those from an accelerator tunnel - are studied. It is shown that hadron, electron and muon colliders are similar and very different at the same time with respect to background origin, integrated radiation levels and instantaneous rates of particles in the detectors.

1. INTRODUCTION

The high physics potential of future hadron, e^+e^- and $\mu^+\mu^-$ colliders comes from the high luminosity ($\mathcal{L} \approx 10^{34} \text{cm}^{-2}\text{s}^{-1}$) of particle collisions in the TeV energy range. The overall detector performance in this new domain is terribly dependent on the background particle rates in various detector components. The mutual effects of the radiation environment produced by the accelerator and experiments have become one of the key issues in the interaction region and detector development [1–3]. A good analysis of the radiation environment in the experiments at the colliders of the generation to come has been recently performed at the SARE2 workshop at CERN [4–7]. In this paper LHC, NLC and 2×2 TeV $\mu^+\mu^-$ colliders are considered as the best representatives of their classes. Despite different colliding particle types and machine parameters, there are many common features of the background environment in the detectors at these accelerators.

Particles originating from the interaction point (IP) and collision remnants are most often the major source of background and radiation levels in the hadron collider detectors, in the experimental halls and in the final focus triplet. Small aperture collimators on either side of the IP in front of the first low- β quadrupoles are the main way to protect the accelerator components from the intense IP radiation [3]. Shielding around such collimators reduces radiation levels in detectors

and in collision halls. For example, two tungsten collimators followed by lead and steel shielding were embedded into the DØ detector at Fermilab from the very beginning, providing favorable conditions for the experiment.

Beam loss in the IP vicinity is the second background source. The collider detectors sit right on the beam lines, so they unavoidably experience bilateral irradiation by particle fluxes from the accelerator tunnel. Without protection, the number of hits from halo particles in the detector can be equal to or even greater than the number of hits from particles originating from the IP and their products. The reduction of beam loss rates in the interaction region is the most efficient and intelligent way to improve this situation. An additional way is the plugging of the accelerator tunnel at the entrance to the experimental hall. A full calculational study, design and installation of the shielding walls at both ends of the DØ detector hall were recently done at the Tevatron [8] resulting in almost a 10-fold suppression of the accelerator backgrounds.

Temporal considerations in the background analysis are of primary importance [6]. Integrated levels determine radiation damage, ageing and radioactivation of detector components as well as the radiation environment in the experimental hall and its surroundings. High instantaneous particle fluxes complicate track reconstruction, cause increased trigger rates and affect detector occupancy. So, the beam's time structure is a driver in the comparison of expected background environments at different machines.

*Work supported by the U. S. Department of Energy under contract No. DE-AC02-76CH03000.

Table 1
Collider parameters and calculated integrated and *effective* luminosities

Parameters	LHC	NLC-500	NLC-1000	$\mu^+\mu^-$
E_{cm} (TeV)	14	0.5	1	4
\mathcal{L} ($10^{34}\text{cm}^{-2}\text{s}^{-1}$)	1	0.71	1.45	4.55
Rep. rate f (Hz)	-	180	120	4.04×10^4
Particles/bunch (10^{11})	1	0.07	0.11	20
Bunch/RF pulse	-	90	75	1
Bunch separation (ns)	25	1.4	1.4	18.6×10^3
Yearly \mathcal{L}_y (fb^{-1})	100	71	145	455
σ_h (μb)	80×10^3	0.045	0.034	0.054
Δt_d or bunch train length (ns)	300	126	105	-
\mathcal{L}_{eff} (cm^{-2})	3.00×10^{27}	3.94×10^{31}	1.21×10^{32}	1.13×10^{30}
$(\sigma_h \times \mathcal{L}_y)/(\sigma_h \times \mathcal{L}_y)_{LHC}$	1	4.00×10^{-7}	6.16×10^{-7}	3.07×10^{-7}
$(\sigma_h \times \mathcal{L}_{eff})/(\sigma_h \times \mathcal{L}_{eff})_{LHC}$	1	7.39×10^{-3}	1.71×10^{-2}	2.54×10^{-4}

2. PARAMETERS AND SOURCES

The parameters of three types of future colliders relevant to the problem under consideration are presented in Table 1. The integrated luminosities, which determine the long-term accumulated effects, are obtained from the design peak values by multiplying by 10^7 s - the standard detector year. The *instantaneous* or *effective* luminosity, which determines the detector performance, is defined for the amount of radiation in the detector active element over the drifting time Δt_d or the bunch train length, whichever is smaller [6]. Collider detector elements most susceptible to occupancy problems have the drifting/integration time in the 40 to 300 ns range. Taking conservatively $\Delta t_d = 300$ ns, one gets $\mathcal{L}_{eff} = \mathcal{L} \times \Delta t_d$ for LHC and $\mathcal{L}_{eff} = \mathcal{L}/f$ for the other colliders, where f is the repetition rate. The NLC $\gamma\gamma$ mode is 10 to 20 times worse compared to the e^+e^- one because of the large backscattered laser cross-section [6]. Multiplying the above luminosities by the appropriate hadron production cross-sections, one can compare pp , e^+e^- and $\mu^+\mu^-$ collisions as a source of background. The last two lines of Table 1 show that LHC produces at least 10^6 times more background hadrons from the IP annually than the lepton machines. At the same time the *instantaneous* background productions are not so drastically different: the NLC IP production rate is

about 1% of that for LHC, whereas the muon collider rate is 0.025% of the LHC one.

The situation is very different with the accelerator related backgrounds. At hadron colliders this component is due to beam-gas interactions in the beam pipe both in the warm and in the cold sections of the interaction region (IR), and due to quasi-local beam halo loss in the IR components, mainly diffractive protons from another IP and halo tails from the beam cleaning system [3]. The Tevatron experience [4,8] and our studies for the SSC [1-3] and LHC (see below) indicate that although the beam halo induced rates might be rather high they can be suppressed below those from the IP via beam loss reduction in the IR and plugging the tunnel at the entrance to the experimental hall, as mentioned in the Introduction.

At the high-energy lepton colliders the backgrounds generated in the machine are a major concern. The studies performed for NLC [9] and TESLA [10] show that synchrotron radiation and muons produced in beam halo interactions along the lattice create serious background levels in the detectors at linear e^+e^- colliders. These can be reduced with an appropriate final focus region design and a set of collimators. At muon colliders the situation is much worse. Unavoidable $\mu \rightarrow e\nu\bar{\nu}$ decays occurring in the beam-pipe have the potential of killing the concept of the muon collider without a complex of serious measures [11-14].

3. SIMULATIONS

Details of high-energy particle interactions with collider and detector components are described elsewhere [3,6,9,12,14–16]. All the studies of background levels are done with a few well established Monte-Carlo codes. At hadron machines the story starts from the pp collision simulations using, usually, the DTUJET event generator [17], based on the two-component Dual Parton Model which treats both soft (low p_t) and hard (minijet, large p_t) processes in a unified and consistent way. Hadronic and electromagnetic showers in collider detectors, experimental halls and surrounding facilities are simulated in practice with one of the four codes: FLUKA [18], GEANT or its version GCALOR [19], LAHET [20], or MARS [21]. Being coupled with the STRUCT code [22], MARS allows in addition detailed analysis of the beam loss problem with a multi-turn tracking of halo particles in the colliders and treatment of their interactions in the lattice components. The cut-off energies are typically ≤ 0.001 eV for neutrons, as low as 10 keV for γ and e^\pm , and 1 MeV for muons and charged hadrons.

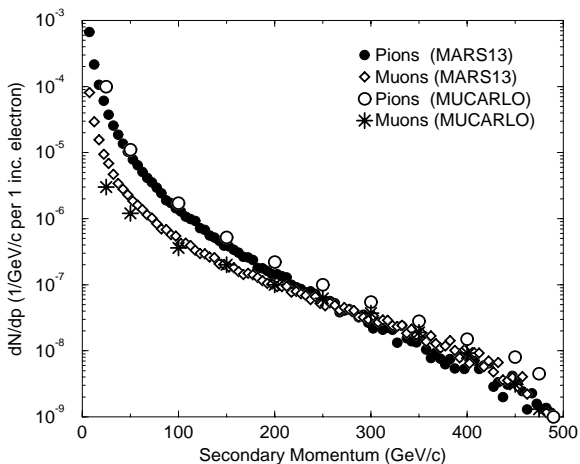


Figure 1. Muon and pion momentum distributions for 500 GeV electrons on a tungsten target, as calculated with the MARS and MUCARLO codes.

Muon background at NLC was studied with the MUCARLO code [9]. STRUCT has been successfully used recently to minimize the expected beam loss rates in NLC and TESLA linear colliders [23]. All studies of the background problem at a 2×2 TeV $\mu^+ \mu^-$ collider [7,12–14] have been performed with the MARS code [21] with one recent attempt to use GEANT for electromagnetic component analysis. Figure 1 shows the secondary muon and pion yields for 500 GeV electrons on a tungsten target 20 radiation lengths thick. The results obtained with two different codes are in good agreement and are of interest for both $e^+ e^-$ and $\mu^+ \mu^-$ colliders. Selected results of recent studies for detectors at LHC, NLC and a muon collider are presented in the next section for IP and beam loss as sources.

4. BACKGROUND LEVELS

Three critical detector regions are paid most attention to: 1) a central tracker with its innermost pixel and strip layers and scintillating fibers or straw tubes at larger radii; 2) endcap and forward calorimeters where the IP background levels reach their maxima; 3) forward muon system interfaced with the machine.

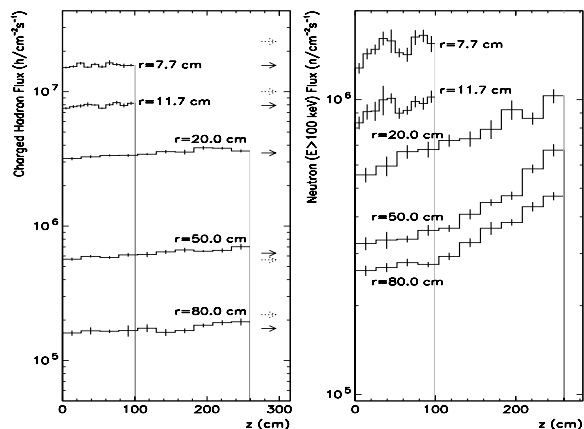


Figure 2. Charged hadron and neutron fluxes at five radii of the CMS central tracker [5].

4.1. LHC

Interaction point. Particle fluxes in the CMS tracking cavity are shown in Figure 2. The charged flux determined by the primary events decrease as $1/r^2$, whereas neutron fluxes are more uniform in the cavity, depending strongly on the calorimeter material. The damage induced in semiconductor components is linearly dependent on the non-ionizing energy loss (NIEL ~ 100 MeV mb [5]), determined by the integrated flux of >100 keV neutrons and charged hadrons. The hit rates are proportional to the charged particle flux (primary and that created by neutrals) in the sensitive volume and are related to the *effective* luminosity. The rates in the end-cap calorimeters are much higher, especially at small radii. Neutron fluxes in the electromagnetic calorimeter can reach high values severely restricting the lifetime of silicon detectors and readout electronics [5]. In the forward muon system, the signal is composed of charged particles, photons with $\sim 1\%$ efficiency and neutrons ($\sim 0.3\%$ efficiency). For the CMS detector, the signal rate ranges from 600 Hz/cm² at $r=1$ m to a few Hz/cm² at $r>5$ m [5]. These values are close to those calculated for ATLAS [6].

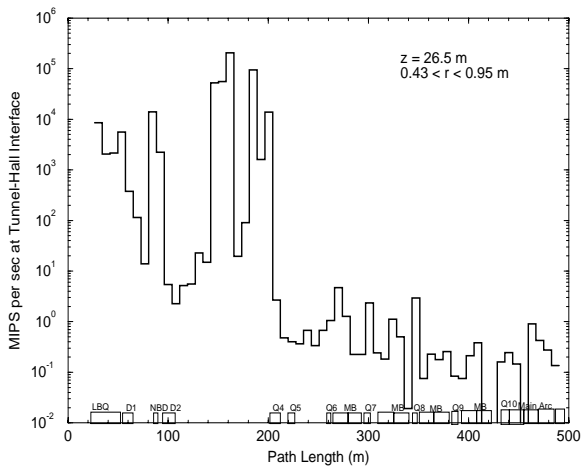


Figure 3. Tagged accelerator background MIP rates entering the CMS detector.

Beam halo. The crucial issue here is the beam loss distribution calculated or assumed in the IR. The source term for the CMS and ATLAS detectors is based on realistic MARS-STRUCT simulations for the entire LHC lattice with model assumptions on the beam-gas interaction rates: 500 m⁻¹s⁻¹ in warm and cold straights and 2×10^4 m⁻¹s⁻¹ in cold arcs. Figure 3 shows background rates tagged for beam loss in the 500 m region. The final focus sections mostly responsible for the backgrounds are clearly seen, indicating the locations to deal with.

Energy spectra of particles coming to the detector from the LHC tunnel are shown in Figure 4 for $r>0.43$ m. The mean energies are 6.6 GeV (μ), 8.1 GeV (h^\pm), 310 MeV (n), 150 MeV (e^\pm), and 30 MeV (γ). The mean distance from the beam axis is 1.5 m, the mean angles are ~ 600 mrad for neutrons and ~ 130 mrad for all other particles. Most of these particles can be intercepted with a concrete plug at the tunnel-hall interface. Muons are an exception, and easily penetrate through shielding, accelerator and detector, creating a rate of a few Hz/cm² in the detector (Figure 5).

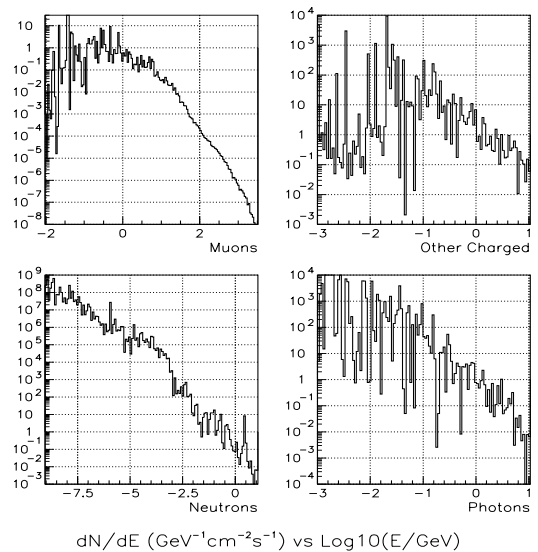


Figure 4. Beam loss induced particle spectra at the entrance to the LHC detector halls.

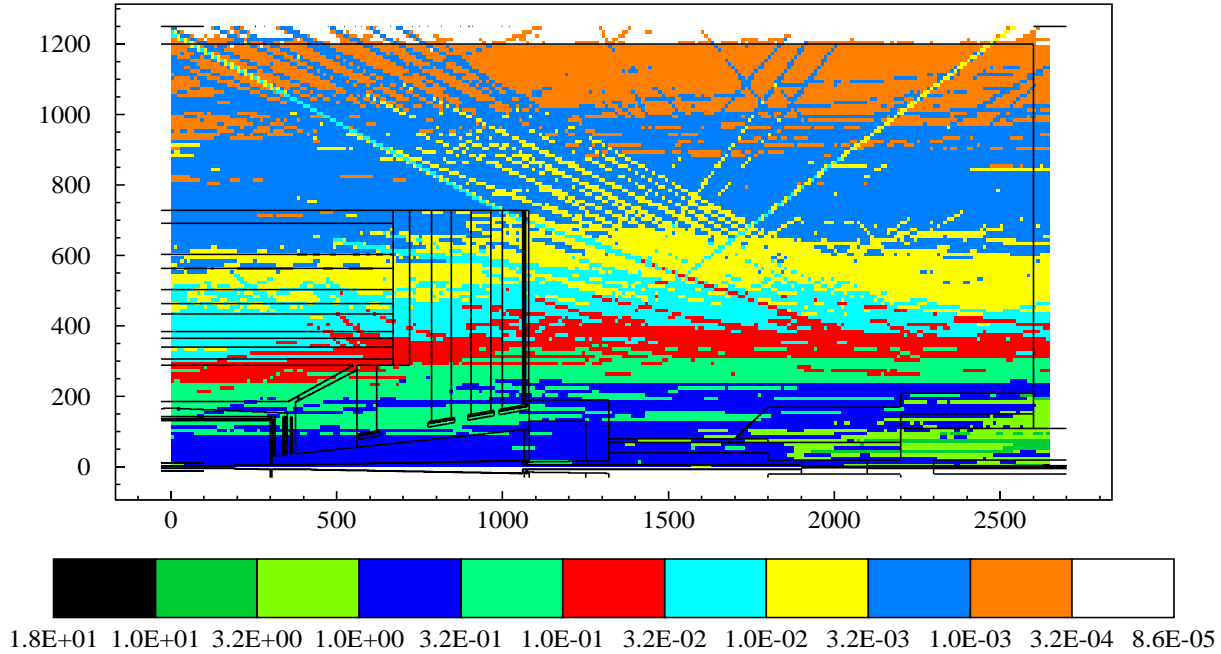


Figure 5. Beam halo induced muon fluence in the CMS detector in units of $10^n \text{cm}^{-2} \text{s}^{-1}$, where the shade indicates the power n .

4.2. NLC

Interaction point. From the standpoint of integrated background, next linear colliders are relatively ‘clean’ machines. As shown in Table 1 the average integrated hadronic fluxes produced at the IP at linear colliders are about six orders of magnitude lower compared to LHC. However, the instantaneous rates are not so drastically different. Figure 6 shows the *effective* h^\pm fluence map calculated in [6] for the NLC $\gamma - \gamma$ option. The authors of [6] conclude that a peak radiation field at the NLC in this mode is about 10% of that at LHC. The e^+e^- option is 10 times better (see Table 1).

Beam halo. Synchrotron radiation, beam-gas and beam halo interactions with the components of the final focus and adjacent sections of the linear colliders create fluxes of muons and other secondaries which can exceed the tolerable levels at a detector by a few orders of magnitude. A multi-stage collimation set and a system of magnetized iron spoilers which fill the tunnel can meet

the NLC design goal of allowing a continuous 1% beam loss, or 10^{10} beam particles per bunch train, resulting in one muon at the detector [9,23]. More work is needed on the contribution of photons, hadrons and low-energy neutrons in all the beam loss mechanisms.

4.3. $\mu^+\mu^-$ COLLIDER

Interaction point. A muon collider is the ‘cleanest’ machine with respect to both integrated and instantaneous particle background from the IP (see Table 1), although there are some indications of the possible importance of coherent pair creation due to beam-beam effects.

Beam halo. With 2×10^{12} muons in a bunch at 2 TeV one has 2×10^5 $\mu \rightarrow e\nu\tilde{\nu}$ decays per meter in a single pass through an interaction region, or 6×10^9 decays per meter per second. Decay electrons with an energy of about 700 GeV and the enormous number of synchrotron photons emitted by these electrons in a strong magnetic field induce electromagnetic showers in the col-

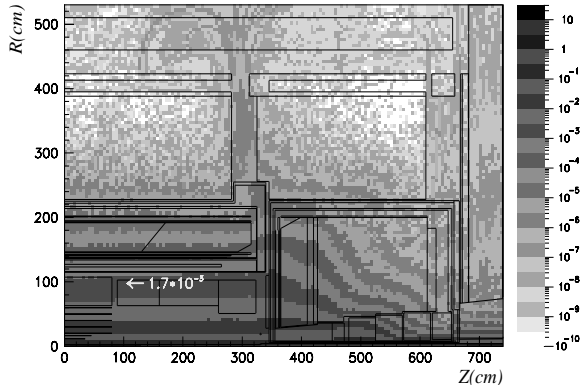


Figure 6. Charged hadron fluence for NLC, integrated over a bunch train $\Delta t = 126$ ns, $\gamma - \gamma$ option, at $\sqrt{s} = 1000$ GeV [6].

lizer and detector components resulting in high background levels. Another contribution comes from beam loss at the limiting apertures.

The hadron, e^\pm , γ and μ fluxes have been examined with MARS in [7,12–14] for a few interaction region and detector configurations. It was found that to suppress the synchrotron generation by decay electrons, the dipole magnets should be kept as far from the IP as possible with the first quadrupole starting not closer than 5–6 m. The most effective collimation includes a limiting aperture about one meter from the IP, with an interior conical surface which opens outward as it approaches the IP (Figure 7). These collimators have the aspect of two nozzles spraying electromagnetic fire at each other, with the charged component of the showers being confined radially by the solenoidal magnetic field and the photons from one nozzle being trapped (to whatever degree possible) by the conical opening in the opposing nozzle. The 250 T/m superconducting low- β quadrupoles have a tapered aperture of about 3.5 cm radius at 6.5 m and twice that at 18 m from IP with ~ 2 cm thick tungsten liner. The 1.2–6.5 m region is occupied with a copper collimator of a conical aperture as shown in Figure 7. Additionally, with a set of catchers at about 60 m from IP, the background rates can be suppressed by a few orders of magnitude.

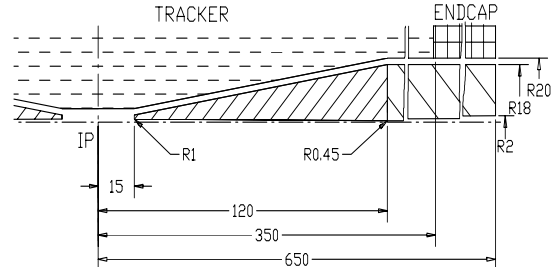


Figure 7. Collimating tungsten nose and copper collimator at a muon collider IP. Dimensions are in centimeters.

Particle spectra in the tracker cavity for the described IR configuration are shown in Figures 8 and 9. All particles over a wide energy range contribute to the background levels. Mean energies of particles in the tracker are given in Table 2.

Table 2

Mean energies of particles in inner tracker for 2 TeV muon decays in the interaction region.

Particle	γ	e^\pm	μ	h^\pm	n
$\langle E \rangle$, MeV	2.5	80	3630	249	0.2

Particle fluxes in the central detector per 2×2 TeV $\mu^+ \mu^-$ bunch crossing are shown in Figure 10 for the most optimal lattice and collimator set. There is a rather uniform distribution of neutrals in the cavity with charged fluxes almost three orders of magnitude lower. Taking into account detector efficiency to n and γ , the expected background hit rate due to $\mu \rightarrow e \nu \bar{\nu}$ decays is about 20 cm^{-2} per a bunch crossing. Figure 11 shows the particle flux maps in the tunnel, collider and detector components.

It is assumed that a reliable beam cleaning system is in the lattice far upstream from the IP. Studies show that the loss of even a small fraction of the beam closer than a few hundred meters to the IP results in backgrounds in a detector comparable to those from $\mu \rightarrow e \nu \bar{\nu}$ decays.

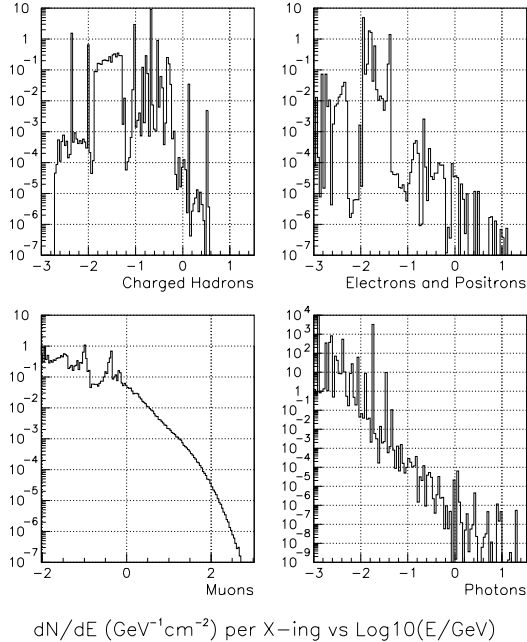


Figure 8. h^\pm, e^\pm, μ and γ spectra in central tracker for 2 TeV muon decays in the IR.

5. CONCLUSIONS

Background particle spectra and space distributions are not very different in similar detector configurations at the LHC, NLC and $\mu^+\mu^-$ colliders (compare, e. g., Figures 4, 8 and 9, and mean particle energies). Expected background levels are summarized in Table 3 for interaction points as a source and in Table 4 for the accelerator backgrounds. The integrated fluxes are converted to the NIEL or “equivalent 1 MeV neutron” [5,6] values, and *instantaneous (effective)* fluxes (signals) are defined as the charged particle flux plus $0.003 \times (F_n + F_\gamma)$. One should stress again that the integrated backgrounds originating from the beam-beam collision points are many orders of magnitude lower for the lepton machines compared to LHC with the *instantaneous* rates at a few % level of the LHC values. Even

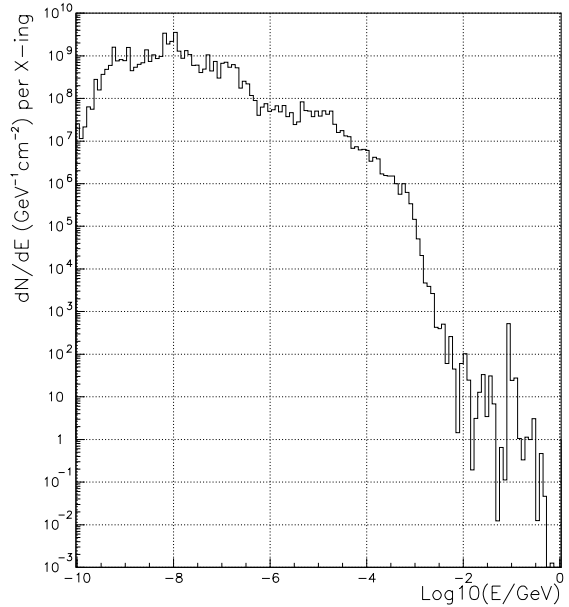


Figure 9. Neutron spectrum in central tracker for 2 TeV muon decays in the IR.

with the sophisticated protective measures, both integrated and *instantaneous* accelerator related backgrounds at muon colliders are much higher than those at the other colliders, being comparable to the LHC IP-produced backgrounds. It means that the same detector technology (pixelated silicon devices, “smart” pixels, scintillating fibers etc.) can be used at these machines. Fine segmentation of the electromagnetic calorimeters at $\mu^+\mu^-$ colliders is a way to deal with the huge energy flux of background particles [12].

6. ACKNOWLEDGMENTS

I express my gratitude to D. Cline, A. Ferrari, M. Huhtinen, R. Noble, R. Palmer and A. Tollestrup for useful discussions.

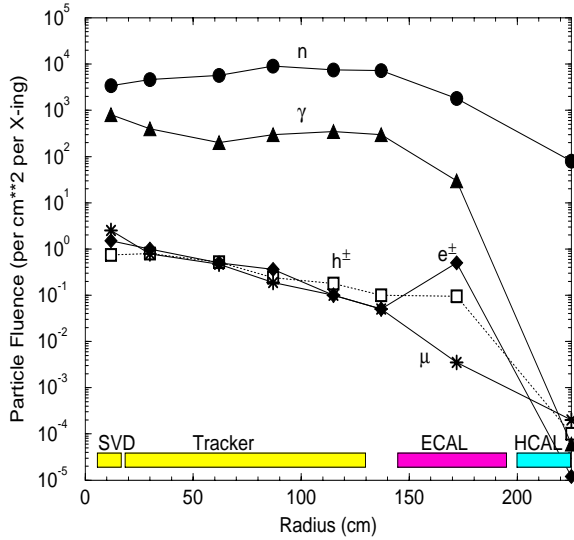


Figure 10. Particle flux radial distributions in a $\pm 1.2\text{m}$ detector region around the IP per $2 \times 2\text{ TeV } \mu^+ \mu^-$ bunch crossing.

Table 3

Background fluxes (cm^{-2}) from the IP accumulated over 1 year (1) and *effective* (2) in central tracker, endcap calorimeter and forward muon spectrometer at different radii

Detector	r (cm)	LHC	NLC	$\mu^+ \mu^-$
(1)				
Tracker	30	2×10^{13}	10^7	6×10^6
ECAL	50	10^{14}	10^8	10^8
Forward	100	10^{11}	5×10^3	8×10^3
(2)				
Tracker	30	0.6	0.01	2×10^{-4}
ECAL	50	0.9	0.8	2×10^{-2}

Table 4

Accumulated over 1 year and *effective* accelerator related fluxes (cm^{-2}) in detector components at $r = 50\text{ cm}$, with all the protective measures on

	LHC	NLC-1000	$\mu^+ \mu^-$
Integrated	10^8	1.6×10^6	4×10^{14}
Effective	3×10^{-6}	10^{-3}	20

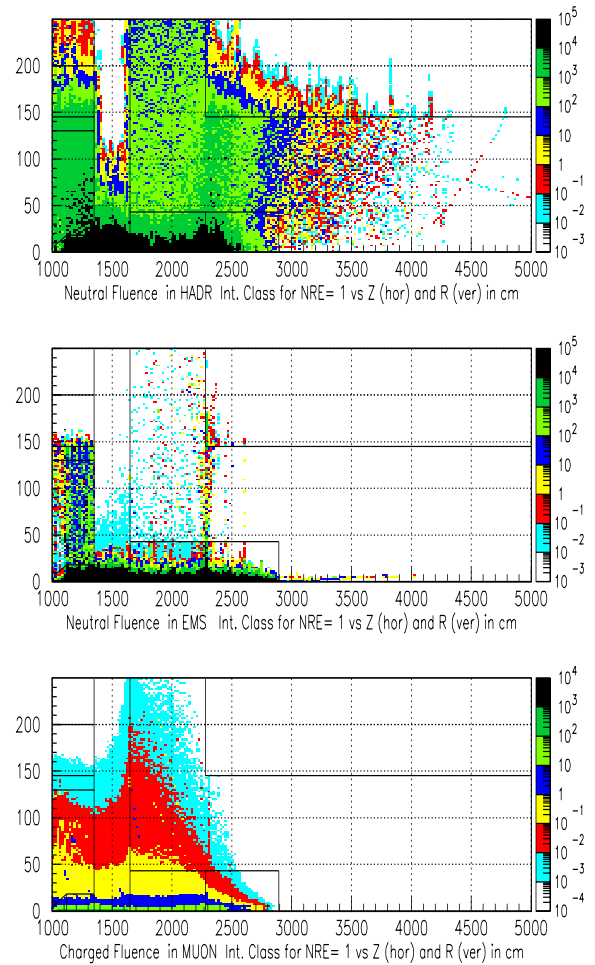


Figure 11. Particle fluxes in the vicinity (2.5m in radius and 50 m long) of $2 \times 2\text{ TeV } \mu^+ \mu^-$ IP (at $z=10\text{ m}$ in the plots). The units are 10^n cm^{-2} per bunch crossing, where the shade indicates the power n . From top to bottom: n , γ and μ .

REFERENCES

1. M. Diwan, Y. Fisyak, N. Mokhov et al., ‘Radiation Environment and Shielding for the GEM Experiment at the SSC’, SSCL-SR-1223 (1993).
2. N. V. Mokhov, ‘Accelerator/Experiment Interface at SSC’, in Proc. of the Workshop on Simulating Accelerator Radiation Environments (SARE), Santa Fe, January 1993, pp. 12–26, LA-12835-C, UC-414 (1994).
3. N. V. Mokhov, ‘Accelerator/Experiment Interface at Hadron Colliders: Energy Deposition in the IR Components and Machine Related Background to Detectors’, Fermilab-Pub-94/085 (1994).
4. N. V. Mokhov, ‘Optimization of the Radiation Environment at the Tevatron’, in *Proc. of the 2nd Workshop on Simulating Accelerator Radiation Environments (SARE2)*, CERN, Geneva, October 1995.
5. M. Huhtinen, ‘Radiation Environment Simulations for the CMS Detector’, *ibid.*
6. R. Engel, A. Ferrari, P. R. Sala, and J. Ranft, ‘Radiation Problems at Linear e^+e^- Colliders’, *ibid.*
7. N. V. Mokhov, ‘The Radiation Environment at Muon Colliders’, *ibid.*
8. J. Butler, D. Denisov, T. Diehl, A. Drozhdin, N. Mokhov, and D. Wood, ‘Reduction of Tevatron and Main Ring Induced Backgrounds in the DØ Detector’, Fermilab-FN-629 (1995).
9. L. P. Keller, ‘Muon Background in a 1 TeV Linear Collider’, SLAC-PUB-6385 (1993).
10. D. Schulte, ‘Backgrounds in the TESLA Interaction Region’, DESY, 1995.
11. ‘Physics Potential and Development of $\mu^+\mu^-$ Colliders’, Sausalito-94, ed. by D. Cline, *AIP Conference Proceedings* **352** (1996).
12. G. W. Foster and N. V. Mokhov, ‘Backgrounds and Detector Performance at a 2×2 TeV $\mu^+\mu^-$ Collider’, in [11] pp. 178–190; also Fermilab-Conf-95/037 (1995).
13. N. M. Gelfand and N. V. Mokhov, ‘ 2×2 TeV $\mu^+\mu^-$ Collider: Lattice and Accelerator-Detector Interface Study’, in *Proc. of 1995 Particle Accelerator Conference*, Dallas, May 1995; also Fermilab-Conf-95/100 (1995).
14. N. V. Mokhov and S. I. Striganov, ‘Simulation of Backgrounds in Detectors and Energy Deposition in Superconducting Magnets at $\mu^+\mu^-$ Colliders’, in *Proceedings of the 9th Advanced ICFE Beam Dynamics Workshop: Beam Dynamics and Technology Issues for $\mu^+\mu^-$ Colliders*, Montauk, NY, October 15–20, 1995; also Fermilab-Conf-96/011 (1996).
15. N. V. Mokhov, *Sov. J. Part. Nucl.*, **18** (1987) 408–426.
16. A. N. Kalinovskii, N. V. Mokhov, and Yu. P. Nikitin, ‘Passage of High-Energy Particles through Matter’, AIP, NY (1989).
17. P. Aurenche, F. Bopp, R. Engel, D. Pertermann, J. Ranft, S. Roesler, *Comp. Phys. Com.*, **83** (1994) 107.
18. A. Fasso, A. Ferrari, J. Ranft, and P. R. Sala, ‘An Update about FLUKA’, in *Proc. of the 2nd Workshop on Simulating Accelerator Radiation Environments (SARE2)*, CERN, Geneva, October 1995.
19. C. Zeitnitz and T. Gabriel, *Nucl. Instruments and Methods*, **A349** (1994) 106.
20. R. E. Prael and H. Lichtenstein, ‘User Guide to LCS: The LAHET Code System’, LA-UR-89-3014, Los Alamos (1989).
21. N. V. Mokhov, ‘The MARS Code System User’s Guide, Version 13(95)’, Fermilab-FN-628 (1995).
22. I. Baishev, A. Drozhdin, and N. Mokhov, ‘STRUCT Program User’s Reference Manual’, SSCL-MAN-0034 (1994).
23. A. Drozhdin and N. Mokhov, ‘Comparison of the TESLA and NLC Beam Collimation Systems’, presented at the NLC Collaboration Meeting, SLAC, February 1996.